A Novel Figure-Eight Coil for Skin Imaging at 7T

S. Maderwald[1,2], S. Orzada[1,2], A. K. Bitz[1,2], O. Kraff[1,2], I. Brote[1,2], J. M. Theysohn[1,2], M. E. Ladd[1,2], S. C. Ladd[1,2], and H. H. Quick[1,2]

[1]Erwin L. Hahn Institute for MRI, Essen, Germany, [2]Department of Diagnostic and Interventional Radiology and Neuroradiology, University Hospital Essen, Essen, Germany

Introduction:

Noninvasive skin imaging requires very high spatial resolution and high SNR in a FOV on the order of 10 x 10 cm^2 coupled with an acceptable scan time. These requirements are mandatory for characterization of healthy skin, inflammatory skin diseases, and differentiation of skin tumors. To image such microscopic structures within the human skin in vivo, special coil setups are used and have already been employed at 1.5T and 3T [1, 2], and even at 7 T [3]. The purpose of the present study was to design a new high-SNR surface coil with an extended FOV but bounded penetration depth for 7 T, to employ it in a clinically feasible protocol, and to compare it with a standard loop coil approach [3].

Fig. 1: Custom-built figure-eight transmit/receive skin coil with a quadratic inner surface area of 7 x 7 cm^2.

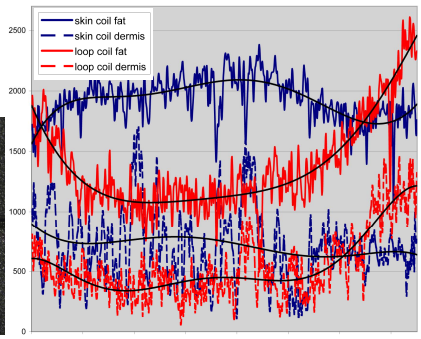

Fig. 2: Signal homogeneity profile comparison of both coils through subcutaneous fat and the dermis. Orientation nearly parallel to the coils – see Fig. 3.

Methods and Materials:

A 7-cm-inner-diameter single-loop transmit/receive coil (Rapid Biomedical, Wuerzburg, Germany) and a custom-built skin transmit/receive coil with a quadratic surface area (inner diameter 7x7 cm^2 (Fig. 1) were used on a 7-Tesla whole-body MRI system (Magnetom 7T, Siemens Healthcare, Erlangen, Germany) equipped with a gradient system capable of 45 mT/m maximum amplitude and a slew rate of 220 mT/m/ms. This gradient performance was mandatory to obtain small FOVs and to accelerate the acquisition speed. The custom-built skin coil consists of two loops with opposing current direction (figure-eight), which renders a penetration depth of approximately 40 mm beyond which virtually no signal can be received. The H-field and therefore the magnetic flux density are oriented parallel to the surface of the coil and are quite homogeneous at a distance of 5 mm to 20 mm from the coil.

The transverse-oriented imaging sequences for in vivo imaging were a T1-weighted spoiled gradient-echo sequence (volume interpolated 3D Flash (VIBE)) (TR/TE = 11.5/5.10 ms , FOV 90 x 90 mm^2, flip 8°, BW 160 Hz/pixel, 128 slices, matrix 512 x 512 interpolated to 1024 x 1024, slice thickness 0.25 mm, in-plane 0.18 x 0.18 mm^2, TA 6:07 min), a T1-weighted "Dixon VIBE" ($TR/TE_1/TE_2$ = 17.5/6.565/11.11 ms, FOV 100 x 100 mm^2, flip 8°, BW 140 Hz/pixel, 92 slices, matrix 512 x 512 interpolated to 1024 x 1024, slice thickness 0.4 mm, in-plane 0.2 x 0.2 mm^2, TA 6:30 min, resulting in fat and water and in- and out-of-phase images), and a T2* weighted SWI sequence (TR/TE = 30/14.1 ms, FOV 119 x 119 mm^2, flip 25°, BW 270 Hz/pixel, 88 slices, matrix 512 x 512 interpolated to 1024 x 1024, slice thickness 0.4 mm, in-plane 0.23 x0.23 mm^2, TA 9:36 min).

The coils were placed directly below of the region of interest (ROI) and fixed only by the weight of the subject on top. Direct comparisons between the coils were performed in four volunteers and evaluated regarding subjective image quality, homogeneity, SNR, CNR, and penetration depth. Quantitative measurements were performed in the dermis and subcutaneous fat in the center and at the edges of the coils. The ROI of the high-resolution in vivo measurements were the calf (n = 2) and the back (n = 2) of the subjects.

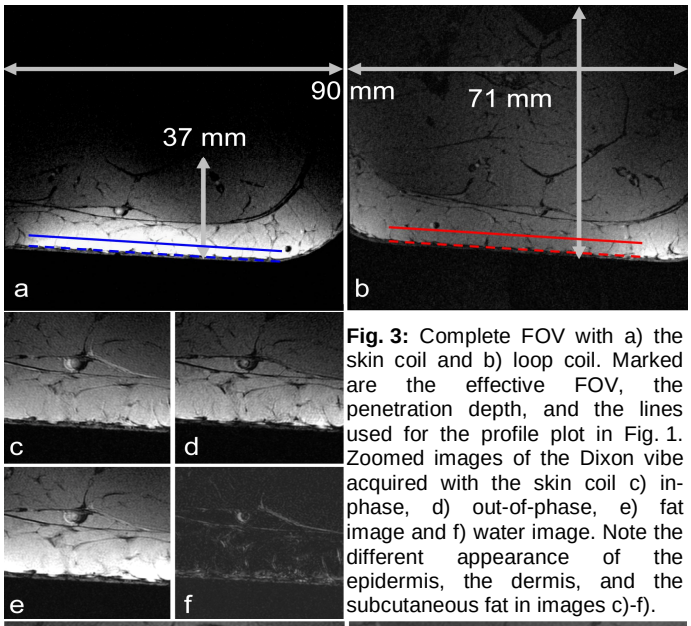

Fig. 3: Complete FOV with a) the skin coil and b) loop coil. Marked are the effective FOV, the penetration depth, and the lines used for the profile plot in Fig. 1. Zoomed images of the Dixon vibe acquired with the skin coil c) in-phase, d) out-of-phase, e) fat image and f) water image. Note the different appearance of the epidermis, the dermis, and the subcutaneous fat in images c)-f).

Results:

Both RF transmit/receive coils provided sufficient SNR and qualitative contrast over the entire ROI in all volunteers in all sequences. Image quality was rated higher for the custom-built coil. Furthermore, the skin coil provides a more homogeneous signal over the FOV (Fig. 2). Additionally, higher SNR values (dermis 9.4 vs. 3.5 and 8.7 vs. 5.2; fat lobule 37.4 vs. 8.6 and 30.3 vs. 16.5) and CNR (fat lobule/dermis 3.9 vs. 2.5 and 3.4 vs. 3.1) were found again for the new coil design [normal VIBE, skin coil vs. loop coil, 1st comparison at center, 2nd comparison at edge]. Finally, the penetration depth of the new coil was effectively reduced in comparison to the loop coil (37 mm vs. 71 mm) (Fig. 3). The coil positioning and examination time of 30 minutes per coil were well tolerated by all subjects. Excellent details of the epidermis, dermis, and the subcutaneous fat were found in all high-resolution T1w MR images (Fig. 3). T2*w images also provided higher SNR for the skin coil and may reveal additional information in diseased skin (Fig. 4).

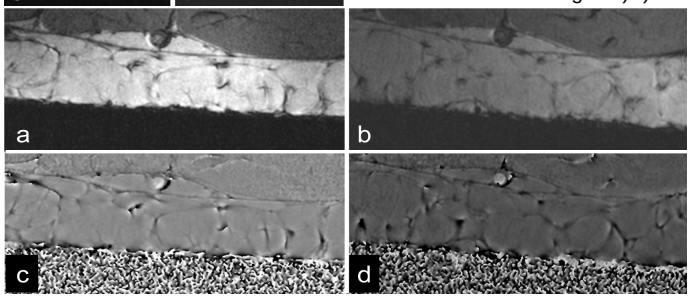

Fig. 4: Magnitude and phase images of the SWI sequence (a, c skin coil; b, d loop coil). Note: the dermis is nearly invisible in magnitude images but visible in phase images due to its very inhomogeneous phase.

Discussion:

These results demonstrate that the new figure-eight skin coil design is capable of rendering increased SNR for high-resolution in-vivo imaging of healthy skin in high-field MR imaging compared to a 'standard' loop coil. This approach circumvents the limitation of measuring with very small surface coils to achieve adequate SNR (as has been shown at 1.5 T and 3 T), as these coils can only depict skin lesions which do not exceed the very small geometry of the sensitive volume (< 2.5 cm). Additionally, the reduced signal penetration depth can be used to reduce the phase FOV and therefore to reduce the overall scan time. Further studies in patients will be performed to assess the potential impact in diseased skin and primarily in cutaneous tumors.

References:

[1] Maderwald, S. et al.: High SNR, Microscopic Imaging of Skin Lesions, ISMRM 2006 Proc. p. 1737; [2] Barral, J.K. et al.: 3T Skin Imaging, ISMRM 2008 Proc. p. 742; [3] Maderwald, S. et al.: Microscopic Skin Imaging at 7T, ISMRM 2008 Proc. p. 1718